Spectral characterization of intermediates in photochemical and dark reactions of hexanuclear rhodium clusters

S. P. Tunik*, A. I. Yarmolenko and A. B. Nikol'skii

Department of Chemistry, St. Petersburg University, Universitetskii pr. 2, St. Petersburg 198904 (Russian Federation)

(Received June 5, 1992; revised October 21, 1992)

Abstract

Irradiation of $Rh_6(CO)_{16}$ in chloroform and dichloromethane at ambient temperature ($\lambda_{irr} > 300$ nm) affords loss of one CO as the only IR detectable photoreaction to yield a product formulated as $Rh_6(CO)_{15}S$ ($S = CHCl_3$, CH_2Cl_2), where the solvent occupies one of the twelve terminal positions in the structure of the parent cluster. Kinetics of the $Rh_6(CO)_{15}S$ reaction with CO have been studied. Species of the same nature were shown to be formed in dark reactions: $Rh_6(CO)_{16} + Me_3NO \xrightarrow[S]{} Rh_6(CO)_{15}S + CO_2 + Me_3N$; $Rh_6(CO)_{15}MeCN \xrightarrow[S]{} Rh_6(CO)_{15}S + MeCN$; $Rh_6(CO)_{16} \xrightarrow[S]{} Rh_6(CO)_{15}S + CO$.

Introduction

The mechanisms of cluster photochemical reactions and the nature of the primary photoproducts formed under UV–Vis irradiation have been reported in a number of articles appearing over the last decade [1–5]. However, detailed investigations involved only trinuclear clusters though photochemistry was widely used in synthetic and catalytic reactions of high nuclear clusters [6–9].

In previous papers [8, 9] we have demonstrated that $Rh_6(CO)_{16}$ photoexcitation in the lowest band of its electronic spectrum is a very effective way to enhance $Rh_6(CO)_{16}$ reactivity in catalytic and substitution reactions. New monosubstituted clusters $Rh_6(CO)_{15}L$ ($L = MeCN$, Py, PPh_3, ethylene, cyclooctene) were obtained in high yield. Terminal alkene isomerization into an inner one was found to be effectively catalyzed by $Rh_6(CO)_{16}$ under photoexcitation or by the labile derivative $Rh_6(CO)_{15}MeCN$ in dark reaction [9]. In both substitution and catalytic processes the same intermediate – coordinatively unsaturated species $\{Rh_6(CO)_{15}\}$ – was postulated. Suggested mechanisms involving $\{Rh_6(CO)_{15}\}$ formation via CO photoejection or dark dissociation of labile MeCN ligand are consistent with the experimental data, but we had not obtained direct evidences for the existence of this species in solution. In the present paper we report the spectroscopic characterization of the intermediates in photochemical and dark reactions of $Rh_6(CO)_{16}$ and its derivative $Rh_6(CO)_{15}MeCN$.

Results and discussion

The electronic spectrum of $Rh_6(CO)_{16}$ in chloroform (Fig. 1), as well as in dichloromethane, displays two overlapping bands centered (in $CHCl_3$) at 258 ($\epsilon_{max} = 4.22\ 10^4\ M^{-1}\ cm^{-1}$) and 310 ($\epsilon_{max} = 1.94\ 10^4\ M^{-1}\ cm^{-1}$) nm. $Rh_6(CO)_{16}$ photolysis in halocarbon solutions with unfiltered radiation of a medium pressure Hg lamp was found to result in an irreversible cluster reaction with the solvent followed by degradation to

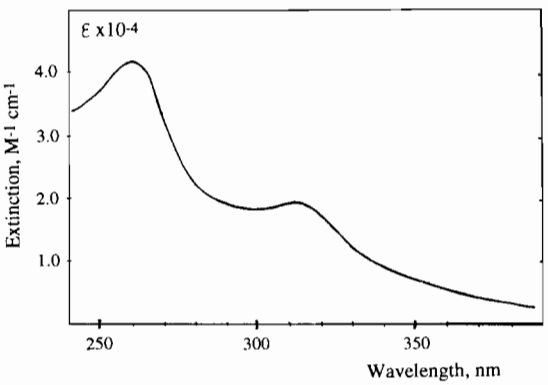

Fig. 1. Electronic absorption spectra of $Rh_6(CO)_{16}$ in chloroform.

*Author to whom correspondence should be addressed.

0020-1693/93/$6.00

unidentified insoluble products. On the contrary, long wavelength excitation ($\lambda_{irr} > 300$ nm) leads to net carbonyl substitution in the presence of MeCN, Py, PPh_3 and alkenes. Continuous photolysis has shown that primary photoproducts generated in the absence of added ligands relax to the parent cluster slowly and we were able to detect the IR characteristics of the intermediates.

Spectral changes in the IR carbonyl region accompanying continuous near-UV irradiation of $Rh_6(CO)_{16}$ chloroform solution are represented in Fig. 2(a). The growth of two weak bands 2132 and 2105 cm^{-1} and long wave shoulders of $Rh_6(CO)_{16}$ bands 2078, 2044, 1810 cm^{-1} is observed. It should be pointed out that the IR spectrum of the photolyte returned to its starting characteristics quantitatively after switching off the irradiation. This means that the process

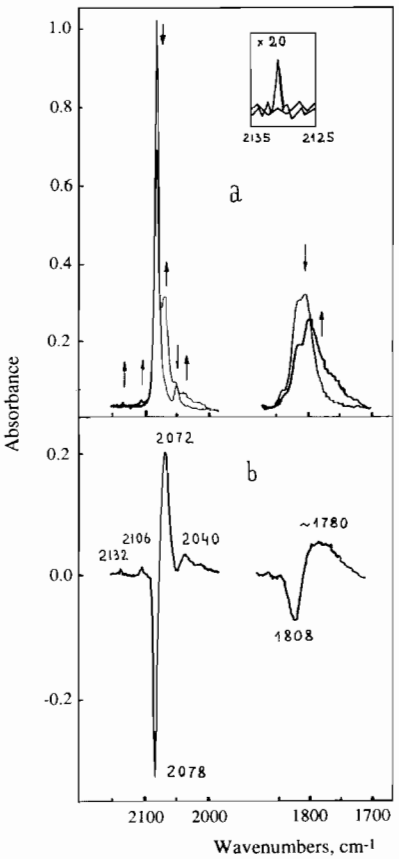

Fig. 2. (a) IR spectral changes accompanying near-UV irradiation ($\lambda_{irr} > 300$ nm) of $Rh_6(CO)_{16}$ chloroform solution. The band at 2132 cm^{-1} (inset) is attributed to free CO. Absorbance in the region 1870–1700 cm^{-1} is shown with three-fold enhancement. (b) Associated IR difference spectrum. The negative absorbance changes are attributed to consumption of $Rh_6(CO)_{16}$ during photolysis, the positive absorbance changes are associated with photoproducts formed in the course of the photoreaction. Corresponding experiments with CH_2Cl_2 solutions revealed the following bands in the positive part of the difference spectrum: 2132vw(free CO absorption), 2103w, 2067m, 2038w, 1794m, br.

$$Rh_6(CO)_{16} \xrightarrow[\text{solvent}]{h\nu} \text{primary photoproducts} \qquad (1)$$

is completely reversible. The IR spectrum of the reaction stationary state depends upon irradiation intensity; the highest degree of $Rh_6(CO)_{16}$ conversion was approximately 30%.

The stationary state spectrum may be considered as a superposition of the $Rh_6(CO)_{16}$ pattern and that of the primary photoproducts. Subtraction of the initial $Rh_6(CO)_{16}$ spectrum gives the spectral curve shown in Fig. 2(b). A very weak band of this difference spectrum at 2132 cm^{-1} was attributed to free CO in solution. The appearance of this band in the photolyte spectrum shows that dissociative loss of CO occurs upon $Rh_6(CO)_{16}$ photoexcitation. Analysis of the remaining part of the difference spectrum shows that $Rh_6(CO)_{16}$ ejects one CO ligand per cluster molecule. In fact, $Rh_6(CO)_{15}L$ derivatives display IR spectra (Fig. 3) which are very close to the positive part of the difference spectrum shown in Fig. 2(b). Coincidence of the number of bands, their relative positions and intensities unambiguously shows that apart from the free CO the only IR detectable photoproduct is the monosubstituted species $Rh_6(CO)_{15}S$ formed in the following process

$$Rh_6(CO)_{16} \underset{\Delta, +CO, -S}{\overset{h\nu, -CO, +S}{\rightleftharpoons}} Rh_6(CO)_{15}S \qquad (2)$$

Solvent molecule substituting CO in $Rh_6(CO)_{15}S$ occupies one terminal position in the structure of the parent cluster $Rh_6(CO)_{16}$ as well as L ligand in

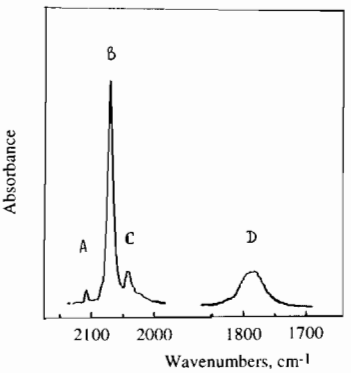

Fig. 3. IR spectra of the monosubstituted $Rh_6(CO)_{15}L$ derivatives in chloroform [8, 9].

Ligand	Band positions, ν_{CO} (cm^{-1})			
	A	B	C	D
Cyclooctene	2104	2072	2040	1796
Ethylene	2106	2072	2044	1798
MeCN	2104	2068	2040	1792
Py	2102	2068	2038	1788
PPh_3	2100	2064	2036	1788

$Rh_6(CO)_{15}L$ derivatives [8]. Slight differences in the band positions for the primary photoproducts generated in $CHCl_3$ and CH_2Cl_2 (Fig. 2) demonstrate the variations in donor–acceptor properties of coordinated solvents.

Thus, $Rh_6(CO)_{16}$ long wavelength excitation results in net ligand dissociation, the Rh_6 metal core remaining intact. This differs significantly from the behavior of dinuclear and trinuclear carbonyls, where corresponding excitation leads mainly to the formation of primary photoproducts with broken metal–metal bonds and corresponding lower nuclearity products [1, 3, 5]. Interpretation of this difference is complicated by the overlapping of the bands in the $Rh_6(CO)_{16}$ electronic absorption spectrum and the impossibility of the selective excitation of a certain transition. However, it can be pointed out that cleavage of any metal–metal bond in the cluster $Rh_6(\mu_3\text{-}CO)_4(CO)_{12}$, involves not only Rh–Rh bond rupture but the distortion or even cleavage of the bond between the μ_3-CO group and the rhodium skeleton. Furthermore, the '$Rh_6(\mu_3\text{-}CO)_4$' framework is a very stable structural unit which remains intact in most of the $Rh_6(CO)_{16}$ reactions studied [8–12].

Chloroform and dichloromethane are weakly bonded ligands and photogenerated $Rh_6(CO)_{15}S$ species in consistency with the formulation react readily with deliberated CO affording the parent $Rh_6(CO)_{16}$ cluster. The considerable amount of $Rh_6(CO)_{15}S$ accumulated in the course of continuous photolysis and the relatively low rate of its interaction with CO allowed us to study the kinetics of this reaction quantitatively. The reaction course was followed by the IR absorbance recording at 2078 cm^{-1} – D_{2078} (the maximum of the most intense $Rh_6(CO)_{16}$ absorption band). The changes of D_{2078} in a typical run are shown in Fig. 4. The initial drop of absorbance is due to $Rh_6(CO)_{16}$ conversion into $Rh_6(CO)_{15}S$ ($S = CHCl_3$) under irradiation. When the stationary state of reaction (1) was reached (horizontal part of the curve), the irradiation was switched off and the kinetics of the dark reaction was recorded. The observed changes in concentrations of reaction mixture components were found to be consistent with the second order rate law

$$\frac{d[Rh_6(CO)_{16}]}{dt} = k_2^{obs} X^2 \qquad (3)$$

Here X is the difference between initial and current $Rh_6(CO)_{16}$ concentrations and is equal to the concentrations of both $Rh_6(CO)_{15}S$ and free CO. Observed and calculated dependences of D_{2078} versus time and the corresponding linearized plot X^{-1} versus time are given in Fig. 5.

Second order rate constant (k_2^{obs}) was found to be $(7.3 \pm 1.3)\ 10^{-2}$ and $(10.3 \pm 2.8)\ 10^{-2}\ M^{-1}\ s^{-1}$ for $S = CHCl_3$ and CH_2Cl_2, respectively. The following reaction scheme

$$Rh_6(CO)_{15}S \underset{k_S}{\overset{k_{-S}}{\rightleftharpoons}} \{Rh_6(CO)_{15}\} \xrightarrow[k_{CO}]{+CO} Rh_6(CO)_{16} \qquad (4)$$

and corresponding rate law

$$\frac{d[Rh_6(CO)_{15}S]}{dt} = \frac{d[Rh_6(CO)_{16}]}{dt} = \frac{k_{CO}[CO]k_{-S}[Rh_6(CO)_{15}S]}{k_S - k_{CO}[CO]} \qquad (5)$$

fits well to the obtained kinetic data; provided that $k_S \gg k_{CO}[CO]$. In this case eqn. (5) is reduced to

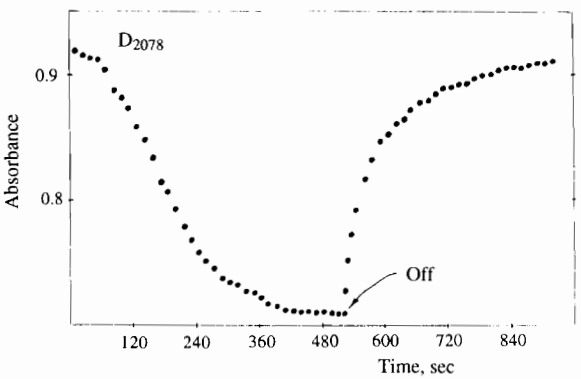

Fig. 4. Typical changes in absorbance of $Rh_6(CO)_{16}$ chloroform solution at 2078 cm^{-1} (D_{2078}) in the course of photolysis followed by the dark reaction of the photoproducts yielding the parent cluster. 'Off' denotes the point of the irradiation switching off.

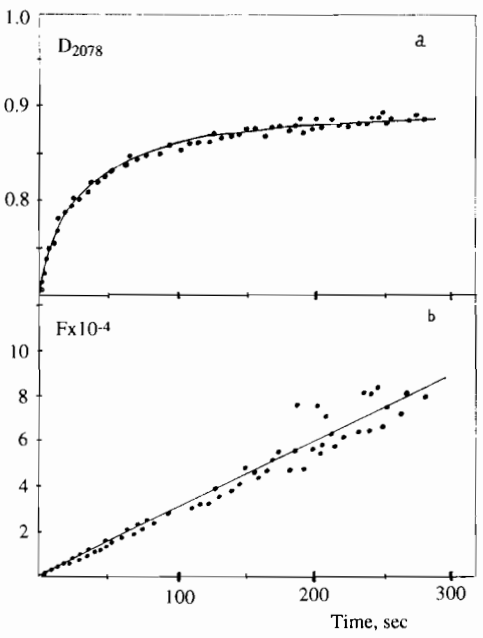

Fig. 5. (a) Typical dependence of $Rh_6(CO)_{16}$ absorbance at 2078 cm^{-1} (D_{2078}) vs. time for the reaction of photochemically generated species $Rh_6(CO)_{15}S$ ($S = CHCl_3$) and CO. (b) Corresponding linearized plot in the second order reaction coordinates. $F = 1/\{[Rh_6(CO)_{16}]_{final} - [Rh_6(CO)_{16}]_{current}\}$.

$$\frac{d[Rh_6(CO)_{16}]}{dt} = \frac{k_{CO}k_{-S}}{k_S}[CO][Rh_6(CO)_{15}S] \quad (6)$$

and consequently $k_{CO}k_{-S}/k_S = k_2^{obs}$.

The following reaction scheme summarizes our current understanding of $Rh_6(CO)_{16}$ photosubstitution processes

$$Rh_6(CO)_{16} \xrightarrow{h\nu} \{Rh_6(CO)_{15}\} \underset{-S}{\overset{+S}{\rightleftharpoons}} Rh_6(CO)_{15}S$$

$$\{Rh_6(CO)_{15}\} \xrightarrow{+CO} Rh_6(CO)_{16}$$

$$\{Rh_6(CO)_{15}\} \xrightarrow{+L} Rh_6(CO)_{15}L$$

where the primary photoreaction is CO dissociation giving the coordinatively unsaturated intermediate $\{Rh_6(CO)_{15}\}$ which yields in the competitive processes more stable solvated $Rh_6(CO)_{15}S$ species, the parent cluster, and substituted derivatives $Rh_6(CO)_{15}L$.

The quantum yield of the photosubstitution reaction for L = MeCN in chloroform was found to be 0.062 ± 0.003 ($[Rh_6(CO)_{16}] = 2.0$–$2.2\ 10^{-4}$ M [MeCN] = 1.0 M).

It is interesting to compare the spectral characteristics of $Rh_6(CO)_{15}S$ obtained in the photochemical experiments with those of solvated coordinatively unsaturated species generated in some independent way. Such a method is a cluster reaction with trimethylamine *N*-oxide widely exploited in carbonyl substitution reactions of the type

$$M_x(CO)_y + Me_3NO + L \longrightarrow M_x(CO)_{y-1}L + Me_3N + CO_2 \quad (7)$$

The mechanism of this reaction suggested earlier [13, 14] involves Me_3NO nucleophilic attack on a coordinated CO group, formation of the good leaving group CO_2 and generation of a coordinatively unsaturated intermediate $\{M_x(CO)_{y-1}\}$. However, in the presence of an entering ligand a fast substitution reaction occurs and no direct information about the spectral characteristics and reactivity of the intermediate was obtained. We carried out the corresponding reaction of the $Rh_6(CO)_{16}$ cluster with Me_3NO in the absence of substituting ligands to detect and characterize $Rh_6(CO)_{15}S$ species using IR spectroscopy.

The amount of added Me_3NO was approximately 40% compared to that of $Rh_6(CO)_{16}$ to avoid second CO group oxidation in the cluster molecule. The IR spectral changes accompanying Me_3NO addition (Fig. 6(a)) are similar to those observed in continuous photolysis experiments. The product formed in the former reaction was found to be sufficiently stable so we obtained a difference spectrum corresponding to $Rh_6(CO)_{15}S$ species (Fig. 6(b)). The characteristics of this spectrum coincide with those of the intermediate

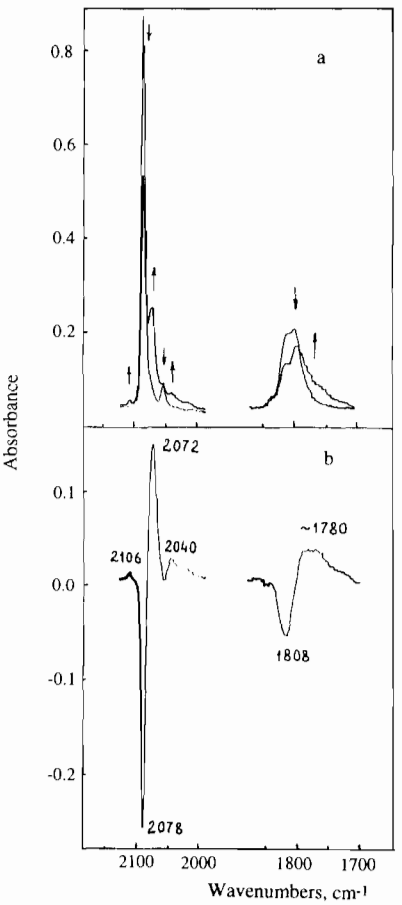

Fig. 6. (a) IR spectral changes accompanying Me_3NO addition to $Rh_6(CO)_{16}$ chloroform solution. Absorbance in the region 1870–1700 cm^{-1} is shown with two-fold enhancement. (b) Associated IR difference spectrum. The negative absorbance changes are attributed to consumption of $Rh_6(CO)_{16}$, the positive absorbance changes are associated with the formation of $Rh_6(CO)_{15}S$ product.

generated in the photochemical reaction. This observation shows the intermediacy of $Rh_6(CO)_{15}S$ both in photochemical and Me_3NO initiated substitution reactions.

Another method of $Rh_6(CO)_{16}$ activation in substitution reactions is a carbonyl ligand exchange for labile acetonitrile in the cluster coordination sphere [8, 9]. It has been shown that the $\{Rh_6(CO)_{15}S\}$ species is formed upon dissociation of acetonitrile from $Rh_6(CO)_{15}NCMe$ in chloroform solution, the solvated species presumably being the intermediate in the NCMe substitution for another ligand. $Rh_6(CO)_{15}S$ formation was detected by an IR spectroscopic study of the following equilibrium

$$Rh_6(CO)_{15}NCMe \underset{-S}{\overset{+S}{\rightleftharpoons}} Rh_6(CO)_{15}S + NCMe \quad (8)$$

S = $CHCl_3$

In the absence of added acetonitrile the equilibrium is slightly shifted to the right. Addition of acetonitrile shifts the reaction almost completely to the starting compound. The corresponding differential spectrum was obtained (see 'Experimental'). All parameters of this spectrum coincide with those obtained for $Rh_6(CO)_{15}S$ species generated in the photochemical experiments and in the chemical oxidation of coordinated carbonyl.

Substitution of CO in $Rh_6(CO)_{16}$ without activation of the parent cluster is a very slow process at room temperature and usually is not applied in the synthesis of substituted derivatives. However, this process is of interest from the mechanistical point of view. We have studied $Rh_6(CO)_{16}$ dark reaction with acetonitrile

$$Rh_6(CO)_{16} + NCMe \longrightarrow Rh_6(CO)_{15}NCMe + CO \quad (9)$$

The reaction was initiated by injection of acetonitrile into the thermostated $CHCl_3$ solution of $Rh_6(CO)_{16}$. Typical $Rh_6(CO)_{16}$ concentration changes are shown in Fig. 7. Observed experimental dependence consists of two parts: initial fast decline in the starting cluster concentration and the following slow reaction corresponding to the linear plot in {ln[$Rh_6(CO)_{16}$]–time} coordinates. Such a complex reaction can be explained using the general reaction scheme given below.

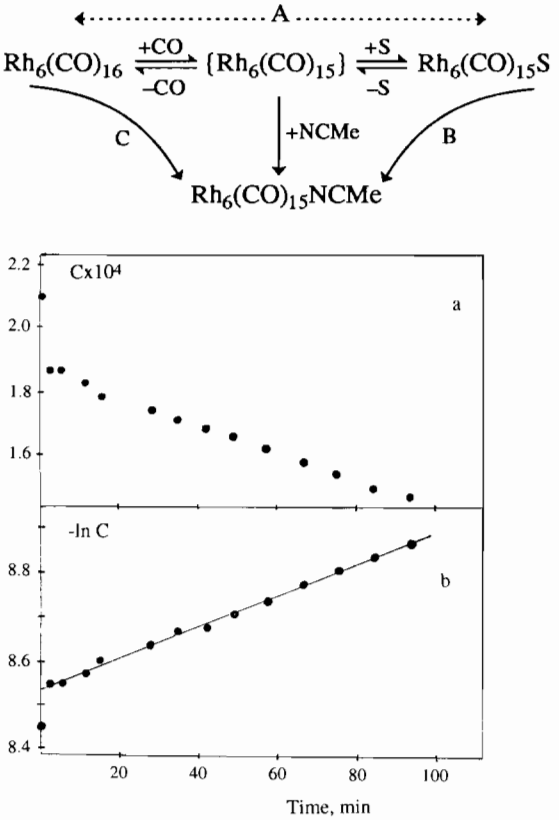

Fig. 7. (a) Typical dependence of $Rh_6(CO)_{16}$ concentration (C) vs. time for the reaction of $Rh_6(CO)_{16}$ with acetonitrile in chloroform solution. (b) Corresponding linearized plot in the first order reaction coordinates.

The initial jump of the reaction component concentrations (decrease in the starting cluster concentration and increase in that of the product) is easily explained if the dissociation preequilibrium (A) is taken into consideration. Fast initial formation of $Rh_6(CO)_{15}NCMe$ is connected with reaction path B, the rate of solvated species reaction with acetonitrile being very high. It should be noted that the $Rh_6(CO)_{15}S$ species has spectral features which are very close to those of $Rh_6(CO)_{16}$ in the region used for the calculations of the concentrations. Hence, the initial decline in $Rh_6(CO)_{16}$ concentration shown in Fig. 7 should be attributed to $Rh_6(CO)_{15}S$ consumption. It is also worth noting that the initial spectral curve does not pass through the isosbestic points which remaine valid for the remaining curves corresponding to the linear part of the plot given in Fig. 7. This fact is also explained by the existence of the third component, $Rh_6(CO)_{15}S$, in the initial reaction mixture. The linear part of the kinetic curve (Fig. 7) is connected with the reaction path C, $Rh_6(CO)_{15}NCMe$ formation from the parent cluster being consistent with the following rate law

$$\frac{d[Rh_6(CO)_{16}]}{dt} = k^{obs}[Rh_6(CO)_{16}] \quad (10)$$

The first order rate constant was found to be independent of the entering ligand concentration and the experimental data fit well to the usual dissociative reaction mechanism. The value of k^{obs} was calculated using the slope of the linear part of the experimental dependence and is equal to 2.9 ± 0.2 (40 °C) and 4.8 ± 0.2 (45 °C) min^{-1}.

All the facts given above show clearly that the {$Rh_6(CO)_{15}$} species formation is the dominant feature of carbonyl substitution reactions in the $Rh_6(CO)_{16}$ cluster, whatever way of initiation of the process was used. This highly reactive coordinatively unsaturated intermediate cannot be detected directly in solution due to the fast competitive processses of its capture by the solvent, substituting ligand or deliberated CO. However, the product of its reaction with the solvent is much more stable and may be detected and characterized by IR spectroscopy. This is a molecule with a structure resembling that of monosubstituted derivatives $Rh_6(CO)_{15}L$, where the solvent occupies one terminal position of the carbonyl environment in the parent $Rh_6(CO)_{16}$ cluster.

Experimental

Reagents and solvents

$Rh_6(CO)_{16}$ was obtained by refluxing for 5 h a hexane solution of $Rh_4(CO)_{12}$ which was synthesized according to ref. 15. $Rh_6(CO)_{15}NCMe$ was prepared as described

earlier [8]. Reagent grade $Me_3NO \cdot 2H_2O$ was used without further purification. Chloroform and dichloromethane were washed with alkaline aqueous solution and distilled water successively, dried over $CaCl_2$ and distilled from P_4O_{10}. Acetonitrile was distilled from P_4O_{10} until the solvent over P_4O_{10} became colourless. The fraction of 81.6–82.0 °C was taken. Purity of solvents was checked by G.L.C. Solutions were deoxygenated by purging with argon.

Instrumentation and procedures

UV–Vis absorption and IR spectra were recorded on Specord M 40 and Specord M 80 instruments, respectively. A medium pressure Hg-lamp (DRSh-500 W) was used as the light source. Quantum yield of the photoreaction was determined using a ferrioxalate actinometer [16]. Light intensity was typically $<10^{-8}$ einstein/min. Photolysis wavelength ($\lambda_{irr} = 313$ nm) was isolated with a chemical/glass filter [17]. Concentrations of reaction mixture components were calculated from IR spectra in the carbonyl region. Extinction coefficients of $Rh_6(CO)_{16}$ and $Rh_6(CO)_{15}(NCMe)$ clusters in the spectral interval of 2082–2060 cm^{-1} were determined and used in the calculations. These measurements were carried out immediately after the clusters dissolution, 5% of MeCN was added to the $Rh_6(CO)_{15}NCMe$ solution to suppress acetonitrile dissociation.

In a typical run $Rh_6(CO)_{16}$ was dissolved in chloroform or dichloromethane to produce a solution of optical density 0.7–0.9 for its most intense IR absorption band (2078 cm^{-1}) in the carbonyl region. An IR cell (KBr windows, optical path length 0.5–3 mm) with $Rh_6(CO)_{16}$ solution was placed in a Specord M80 cell compartment. The spectrum of the starting solution was recorded in the region 2150–1700 cm^{-1}. UV irradiation was switched on and the reaction was monitored by registration of the 2078 cm^{-1} absorbance. During irradiation the absorbance diminished and became constant within approximately 20 min. When the stationary state was reached, the spectrum of the photolyte in the same region (2150–1700 cm^{-1}) was recorded. The difference spectrum of the photolyte and initial $Rh_6(CO)_{16}$ solution was obtained using standard software of the Specord M80 instrument. Then the irradiation was switched off and absorbance changes at 2078 cm^{-1} were recorded in 'time-drive' regime. Measurements were carried out up to the complete conversion of the photolyte spectral parameters to those of the starting $Rh_6(CO)_{16}$ solution. Changes of $Rh_6(CO)_{16}$ concentration in the course of the photolyte dark relaxation were calculated and the second order rate constant was estimated.

$Rh_6(CO)_{16}$ reaction with trimethylamine N-oxide

A chloroform solution of $Me_3NO \cdot 2H_2O$ (2.8 mg, 0.025 mmol) was added dropwise to a freshly prepared $Rh_6(CO)_{16}$ (60.0 mg, 0.056 mmol) chloroform solution (100 cm^3), under vigorous stirring. The reaction mixture was stirred for 20 min. The difference spectrum of reaction mixture and initial $Rh_6(CO)_{16}$ solution (with correction to dilution) was obtained as described above.

Spectral investigation of the dissociation equilibrium in $Rh_6(CO)_{15}NCMe$ solution

$Rh_6(CO)_{15}NCMe$ was dissolved in chloroform and the spectrum of the prepared solution was recorded in the range 2150–1700 cm^{-1}. Acetonitrile (5%) was then added and the spectrum was registered in the same spectral interval. The difference spectrum was obtained as described above. The following bands were observed in the positive part of this spectrum: 2106w, 2072m, 2041w, 1785w, br.

Dark $Rh_6(CO)_{16}$ reaction with MeCN in chloroform

A chloroform solution of $Rh_6(CO)_{16}$ was placed into a water thermostated (45 °C) reaction vessel. After about 30 min temperature equilibration the spectrum of the initial solution was recorded in the range 2082–2060 cm^{-1} and a certain amount of MeCN was injected. Probes of the reaction mixture were taken out by a syringe at appropriate time intervals and the reaction course was monitored by IR spectral measurements. Concentrations of reaction mixture components were calculated using the values of extinction coefficients at the corresponding wavenumbers; at least 10 points in the 2082–2060 cm^{-1} range were used. Spectral changes in the course of the reaction showed good isosbestic points except for the spectral curve of the initial solution. The dissolution effect upon MeCN injection was accounted for in the calculations.

References

1 J. G. Bentsen and M. S. Wrighton, *J. Am. Chem. Soc., 109* (1987) 4518, 4530.
2 J. G. Bentsen and M. S. Wrighton, *J. Am. Chem. Soc., 106* (1984) 4041.
3 P. C. Ford, A. E. Friedman and D. J. Taube, *ACS Symp. Ser., 333* (1987) 123.
4 A. E. Friedman and P. C. Ford, *J. Am. Chem. Soc., 111* (1989) 551.
5 J. Malito, J. Markievicz and A. Poe, *Inorg. Chem., 21* (1982) 4335.
6 D. Osella, S. Aime, G. Nicola, R. Amadelli, V. Carassiti and L. Milone, *J. Chem. Soc., Dalton Trans.,* (1987) 349.
7 S. P. Tunik, V. R. Krym and A. B. Nikol'skii, *Metallorg. Khim., 3* (1990) 382.
8 S. P. Tunik, A. V. Vlasov, A. B. Nikol'skii, V. V. Kryvikh and M. I. Rybinskaya, *Metallorg. Khim., 3* (1990) 387.
9 S. P. Tunik, A. V. Vlasov, A. B. Nikol'skii, V. V. Kryvikh and M. I. Rybinskaya, *Metallorg. Khim., 4* (1991) 586.

10 B. L. Booth, M. J. Else, R. Fields and R. N. Haszeldine, *J. Organomet. Chem., 27* (1971) 119.
11 D. F. Forster, B. S. Nichols and A. K. Smith, *J. Organomet. Chem., 236* (1982) 395.
12 Z. Hou, Y. Wakatsuki and H. Yamazaki, *J. Organomet. Chem., 399* (1990) 103.
13 J. K. Shen, Y. L. Shi, Y. C. Gao, Q. Z. Shi and F. J. Basolo, *J. Am. Chem. Soc., 110* (1988) 2414.
14 J. K. Shen, Y. C. Gao, Q. Z. Shi and F. J. Basolo, *Inorg. Chem., 27* (1988) 4236.
15 S. Martinengo, P. Chini and G. Giordano, *J. Organomet. Chem., 27* (1971) 389.
16 C. G. Hatchard and C. A. Parker, *Proc. R. Soc. London, Ser. A, 235* (1956) 518.
17 J. F. Rabek, *Experimental Methods in Photochemistry and Photophysics,* Wiley, Part 2, 1982, Ch. 26.